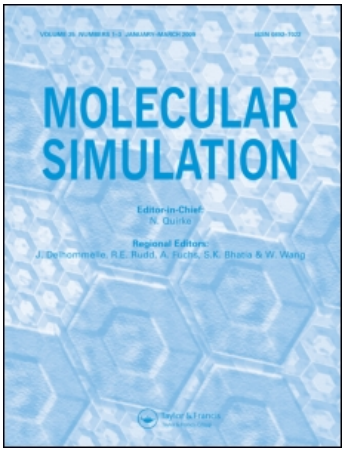

Molecular Simulation
Publication details, including instructions for authors and subscription information:
http://www.informaworld.com/smpp/title~content=t713644482

Heat conduction analysis of nano-tip and storage medium in thermal-assisted data storage using molecular dynamics simulation

X. J. Liu[ab]; J. P. Yang[b]; Y. W. Yang[a]
[a] School of Civil and Environmental Engineering, Nanyang Technological University, Singapore [b] Data Storage Institute, Singapore

To cite this Article Liu, X. J. , Yang, J. P. and Yang, Y. W.(2008) 'Heat conduction analysis of nano-tip and storage medium in thermal-assisted data storage using molecular dynamics simulation', Molecular Simulation, 34: 1, 57 — 63
To link to this Article: DOI: 10.1080/08927020701730401
URL: http://dx.doi.org/10.1080/08927020701730401

Molecular Simulation
Vol. 34, No. 1, January 2008, 57–62

Taylor & Francis
Taylor & Francis Group

Heat conduction analysis of nano-tip and storage medium in thermal-assisted data storage using molecular dynamics simulation

X.J. Liu[ab1], J.P. Yang[b2] and Y.W. Yang[a]*

[a]*School of Civil and Environmental Engineering, Nanyang Technological University, Nanyang Avenue, Singapore, 639798;* [b]*Data Storage Institute, DSI Building, 5 Engineering Drive 1, Singapore, 117608*

(Received 26 July 2007; final version received 6 October 2007)

In the thermal-assisted data storage technologies, the behavior of heat transfer between the nano-tips and the storage medium during thermo-mechanical data bit formation process is a critical factor affecting the areal storage density, data bit writing/reading speed and system reliability. In this paper, the thermal properties of a nano-tip are analyzed using the non-equilibrium molecular dynamics simulation. The simulated results show that the effects of the nano-structural configuration and boundary conditions on the thermal transport are remarkable, which can be attributed to the phonon boundary-scattering and possible phonon spectrum modification. Furthermore, the heat transfer between the nano-tip and the silicon medium film is simulated. The results show that the medium film can be efficiently heated locally with no pressure force. For a tip-medium contact area of 5.31 nm^2, an area of about 95.5 nm^2 on the medium surface can be heated with a temporal resolution of 0.11 ns. This time period is much smaller than the conduction timescale ($\approx 2\,\mu s$) on the nano-tip in the heat-assisted scanning probe-based data storage technology during data bit writing process.

Keywords: heat transfer; nano-tip; molecular dynamics simulation; data storage

1. Introduction

Within a few years, magnetic storage technology is meeting a fundamental challenge, the well-known super-paramagnetic limit. In order to propel the industry to continuously develop new storage technologies for large storage capacity and high data transfer rate, several attractive alternate proposals have been put forward, such as the heat-assisted magnetic recording technology [1] and the heat-assisted scanning probe-based data storage technology [2–5]. In these recording technologies, the behavior of heat transfer in the nano-tips as well as between the nano-tips and the storage medium during thermo-mechanical data bit formation process is a critical factor affecting the areal storage density, data bit writing/reading speed and system reliability. However, the phenomenon has not yet been well understood. In addition, in these systems, the size of nano-tips is comparable to the phonon mean-free path (MFP) and the inter-atomic distances, and the thermal conductivity of nano-tips is much scale-dependent [6]. The measurement of thermal conductivity for the nano-tip remains a challenge for the current experimental techniques. Molecular dynamics (MD) simulation is an ideal tool for addressing such an issue and can provide useful information and in-depth understanding of the nanoscale heat transfer phenomenon during the data recording process.

In this paper, the thermal properties of a nano-tip and the heat transformation between the nano-tip and medium film are investigated using the non-equilibrium molecular dynamics (NEMD) simulation, which relies on imposing a temperature gradient and a heat flux across the simulated system, therefore, is analogous to the experimental situation.

2. Modeling

2.1 Nano-tip structure

Single-crystal Si has a cubic lattice structure, known as the diamond lattice structure, characterized by strong directional bonding, low Poisson's ratio, strong temperature-sensitive yield strength and narrow dislocations with large Peierls–Nabarro forces. The Si atoms touch each other along the four $\langle 111 \rangle$ directions and the nearest-neighbour distance is $(\sqrt{3}/4)a_0$, where a_0 is the lattice constant ($a_0 = 0.543$ nm).

In this paper, a nano-tip with four-side pyramidal shape shown in Figure 1 is studied. Such a tip is convenient to construct using the anisotropic etching process technique. The inclined side face of the nano-tip

*Corresponding author. Email: cywyang@ntu.edu.sg

ISSN 0892-7022 print/ISSN 1029-0435 online

DOI: 10.1080/08927020701730401
http://www.informaworld.com

is determined by a (111) plane in the Si crystal, well defined and yielding very sharp edges. The four adjacent diamond {111} planes form a 60° pyramidal crystal structure where the points of intersection of the planes constitute the vertices of the nano-tip. Therefore, the tip scans over the {100} planes that are parallel to the surface of the medium substrate.

In practice, a perfect 60° pyramid formed from a truncated diamond lattice is unstable at the atomic scale. The atoms on the {111} surfaces of the tip will reconstruct and the apex will evolve into certain curved surface. Furthermore, the tip blunts due to continuous operation and the curvature of the apex is modified with continuous use. Thus, in order to simulate the experimental situation, the first three unit cell layers of the tip apex in the {100} plane will be truncated in the tip model, as shown in Figure 1.

The height of the nano-tip is $10a_0 = 5.43$ nm, consisting of 10 Si (100) unit cell layers stacked upon each other. There are 7×7 atoms on the bottom surface of the tip, which corresponds to a contact area of approximate 5.31 nm^2 ($3\sqrt{2}a_0 \times 3\sqrt{2}a_0$), and 27×27 atoms on the top atom layer of the tip, which corresponds to a contact area of approximate 99.66 nm^2 ($13\sqrt{2}a_0 \times 13\sqrt{2}a_0$). The total number of atoms is 11,890 in the tip model.

2.2 *Nano-film for storage medium*

For simplicity, here we use amorphous silicon nano-film as the storage medium. The overall size of the nano-film is $18a_0 \times 18a_0 \times 2a_0$ including 5184 atoms. The structure of amorphous silicon film is produced by a melt-quench method. The film is annealed at 1600 K for 10 ns. After annealing, almost all point defects such as void and interstitial have disappeared.

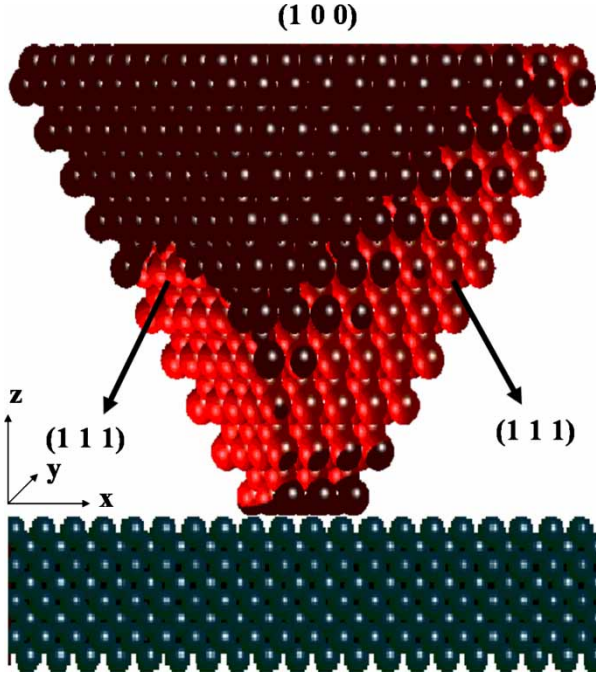

Figure 1. Nano-tip and storage medium film.

3. NEMD simulation for heat transformation

In the NEMD simulation, the Gear's five-value predictor–corrector algorithm is used for the numerical integration of the equations of motion of individual atoms in the nano-tip and medium film. The step time δt is set at 0.57 fs which is short enough to resolve the vibrational motions of the Si atoms. The nano-tip is treated with fixed boundary condition on four (111) side surfaces and with free boundary condition on (100) top and bottom surfaces; the medium film is treated with periodic boundary condition in the x and y directions and with free boundary condition in the z direction.

The Tersoff-type n-body potential [7,8] is employed to describe the interactions between the Si atoms. The total Tersoff energy of the simulated system is expressed in terms of the summation of atomic pair interactions, as a function of the atomic coordinates as follows:

$$V = \sum_{i \neq j} W_{ij} \quad W_{ij} = f_C(r_{ij})[f_R(r_{ij}) + b_{ij} f_A(r_{ij})] \tag{1}$$

$$\begin{aligned} f_R(r_{ij}) &= A \exp(-\lambda r_{ij}) \\ f_A(r_{ij}) &= -B \exp(-\mu r_{ij}) \end{aligned} \tag{2}$$

$$f_C(r_{ij}) = \begin{cases} 1 & r_{ij} \leq R \\ \frac{1}{2} + \frac{1}{2} \cos\left(\frac{r_{ij} - R}{S_{ij} - R_{ij}} \pi\right) & R \leq r_{ij} \leq S \\ 0 & r_{ij} \geq S \end{cases} \tag{3}$$

$$\begin{aligned} b_{ij} &= \chi_{ij} \left(1 + \beta_i^n \zeta_{ij}^n\right)^{-1/2n} \\ \zeta_{ij} &= \sum_{k \neq i,j} f_C(r_{ik}) g(\theta_{ijk}) \end{aligned} \tag{4}$$

$$g(\theta_{ijk}) = 1 + \frac{c^2}{d^2} - \frac{c^2}{d^2 + (h - \cos\theta_{ijk})^2} \tag{5}$$

where V is the system potential energy, W_{ij} is the bond energy for all the atomic bonds, i, j, k label the atoms, r_{ij} is the length of the ij bond, b_{ij} is the bond order term, θ_{ijk} is the bond angle between the bonds ij and ik, f_R represents a repulsive pair potential, f_A represents an attractive pair potential, f_C represents a smooth cutoff function to limit the range of the potential, and ζ_{ij} counts the number of other bonds to atom i besides the ij bond.

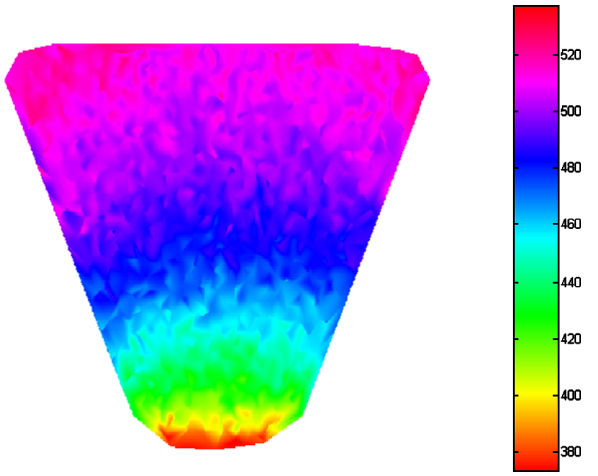

Figure 2. Temperature distribution in nano-tip.

The potential parameters A, B, R, S, χ_{ij}, λ, μ, β, n, c, d, and h are constants which can be found in [7,8].

The thermal conductivity of nano-tip is calculated based on the kinetics theory of gases and the Fourier's law [9] as follows.

$$k(T) = -\frac{J_z}{\nabla T_z} \tag{6}$$

where k is the thermal conductivity, $J_z(= \Delta\varepsilon/A\Delta t)$ is the heat flux vector defined as the amount of heat energy ($\delta\varepsilon$) transferred per unit time (δt) through unit area (A) perpendicular to the direction of the heat flux, and $\nabla T_z = \partial T/\partial z$ is the temperature gradient in the z direction along the tip height. Experimentally, k is typically obtained by measuring the temperature gradient based on a heat flux. Here, it is calculated using the NEMD simulation.

In order to obtain the temperature gradient ∇T_z, the system is divided into j slices along the z direction. The temperature of atoms in the slice is calculated in each iteration. The instantaneous temperature profile in each slice centered at position z can be obtained by

$$T_j(t) = \left\langle \sum_{i=1}^{N_j} m_i v_i^2 \right\rangle 3N_j k_B \tag{7}$$

where $T_j(t)$ is the temperature in the jth slice, m_i and v_i are the mass and velocity of the ith atom, $\langle\ \rangle$ denotes the statistical averaging over the entire simulation duration, N_j is the number of atoms in the jth slice and k_B is the Boltzman constant.

The thickness of slice depends on the size of simulation system. According to the MFP and the average phonon velocity [10], at least 30 atoms are needed in each slice to yield sufficient phonon–phonon scattering events within 1 ns. Furthermore, from the thermodynamic point of view, the temperature is a statistical parameter, which can be defined for any value of N_j at any time t. If the set of atoms is at the equilibrium temperature T, the deviation of $T_j(t)$ will depend on T and the number of atoms: $|T_j(t)/T - 1| = 1/\sqrt{N_j}$ [11]. To obtain a good estimation of $T_j(t)$, N_j has to be adequately large so that $1/\sqrt{N_j}$ is smaller than the desired accuracy. Thus, in this simulation, at least 32 atoms are included in each slice.

The simulation consists of two stages, the energy minimization process and the constant energy process. In the former stage, the system temperature keeps constant by rescaling the velocities of atoms in the system, and the potential energy minimization process is conducted on the system by relaxing the conformation. To keep temperature constant, the velocity adjustment factor, α, is obtained by

$$\alpha^2 = \frac{3nk_B T_{obj}}{\sum_{i=0}^{n} m_i v_{i\_old}^2} \tag{8}$$

$$v_{i-new} = \alpha v_{i\_old} \tag{9}$$

where n is the total number of atoms in the system, T_{obj} is the objective constant temperature, and v_{i_old} and v_{i_new} are the velocities of the ith atom before and after rescaling, respectively. The energy minimization is achieved if the instantaneous variations of the potential energy are less than 1 meV. After this process, the system will reach the equilibrium status.

The later stage is the constant energy process. A heat flux is imposed on the system along the z direction. It can be realized by keeping the temperatures of the hot (T_{hot}) and cold (T_{cold}) thermal reservoirs constant and setting $T_{hot} - T_{cold} = 150$ K in this simulation. The hot and cold thermal reservoirs are located at the top and bottom ends of the nano-tip, respectively. These two constant temperatures can be realized from Equations (8) and (9). In order to eliminate the tendency of the center of mass of the entire system to drift, the velocity-rescaling algorithm of Jund and Jullien [12] is used. During the simulation, the kinetic energies added to the hot thermal reservoir ($\Delta\varepsilon_{hot}$) and removed from the cold thermal reservoir ($\Delta\varepsilon_{cold}$) are calculated. Thus, the heat flux can be obtained from

$$J_z = \frac{\Delta\varepsilon_{hot} + \Delta\varepsilon_{cold}}{2A(z)t}. \tag{10}$$

Since the cross section area $A(z)$ changes along the z direction, Equation (6) can not be used directly. It should be transformed into:

$$\frac{\Delta\varepsilon}{\Delta t}\int_{z_1}^{z_2}\frac{dz}{A(z)} = -\int_{T_{cold}}^{T_{hot}} k(T)\,dT \tag{11}$$

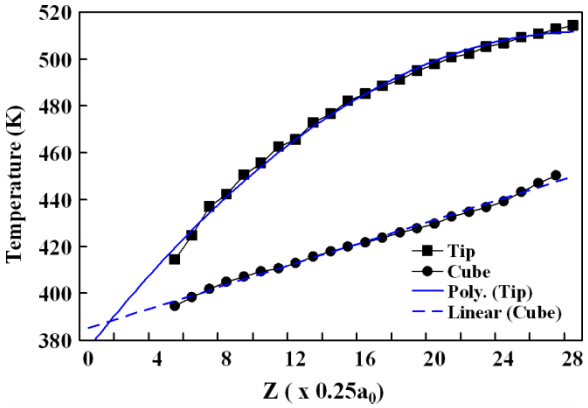

Figure 3. Temperature profiles of nano-tip and nano-cube, represented by full squares and full circles, respectively. The solid line represents the polynomial fitting of the nano-tip temperature profile and the dash line denotes the least-square linear fitting of the nano-cube temperature profile.

$$\frac{\Delta\varepsilon}{\Delta t} = -\frac{\bar{k}}{B}(T_{\text{hot}} - T_{\text{cold}}) \tag{12}$$

where

$$\frac{\Delta\varepsilon}{\Delta t} = \frac{\Delta\varepsilon_{\text{hot}} + \Delta\varepsilon_{\text{cold}}}{2t}, \qquad \bar{k} = -\frac{\int_{T_{\text{cold}}}^{T_{\text{hot}}} k(T)\mathrm{d}T}{T_{\text{hot}} - T_{\text{cold}}},$$

$$B = \int_{z_1}^{z_2} \frac{\mathrm{d}z}{A(z)}$$

and $\bar{k}$ is the integral mean of nano-tip thermal conductivity.

4. Results and discussion

The heat transformation in the nano-tip is firstly simulated. Figure 2 shows a contour plot of the temperature distribution in the nano-tip. It can be found that, at the same high level (shown by dash lines in Figure 2), the temperature of the region near the boundary is a bit higher than that far from the boundary, which is resulted from the fixed boundary conditions. This phenomenon indicates that there exists substantial reflection of phonons and phonon boundary-scattering at the boundary.

Figure 3 shows the temperature profile of the nano-tip along the z direction. Since the cross sectional areas of the tip are not constant, and in order to compare with the

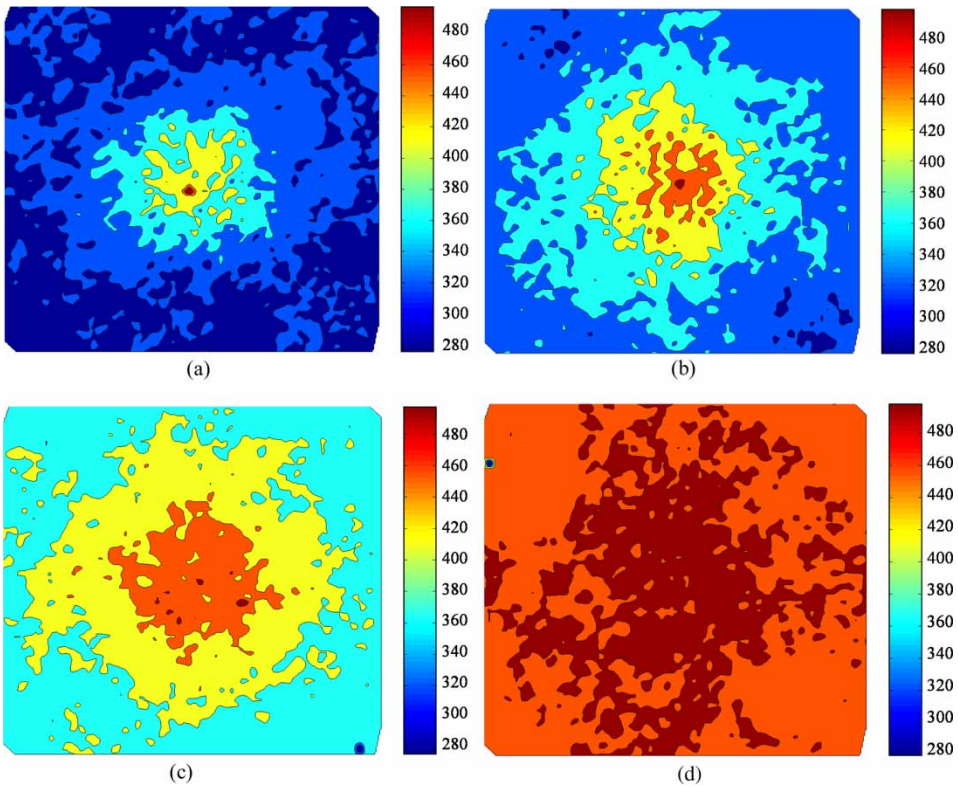

Figure 4. Snapshots of temperature distribution on medium film surface during heat transfer from nano-tip to medium: (a) $t = 0.01$ ns, (b) $t = 0.03$ ns, (c) $t = 0.06$ ns, and (d) $t = 0.10$ ns.

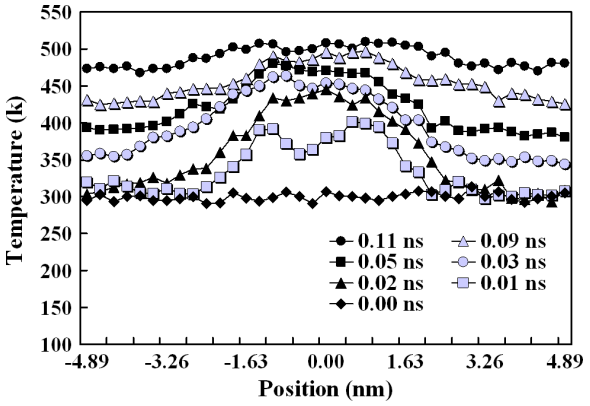

Figure 5. Temperature profiles at the middle section of storage medium along x direction during heat transfer process.

conventional nano-structure configurations, a silicon nano-cube ($10a_0 \times 10a_0 \times 10a_0$) is also simulated with the same simulation conditions as the nano-tip. The temperature profile of the nano-cube is also shown in Figure 3. As expected, it is observed that the temperature of the nano-cube is linearly distributed, and thus, the temperature gradient is constant ($\nabla T_z = 1.7 \times 10^{10}$ K/m in this case) because of the constant cross sectional area. The thermal conductivity of the nano-cube can be calculated based on the Fourier's law as $k \approx 2.7$ W/mk. In contrast, because of the varying cross sectional area, the temperature of the nano-tip is nonlinearly distributed, and the temperature gradient is therefore non-constant. The integral mean of thermal conductivity of the nano-tip is obtained as $\overline{k} \approx 1.1$ W/mk. Furthermore, it can be found that with the increase of the cross sectional area along the z direction, the temperature gradient decreases homologously, which indicates that the finite size and structural configuration effects on thermal transport weaken with the increasing system size.

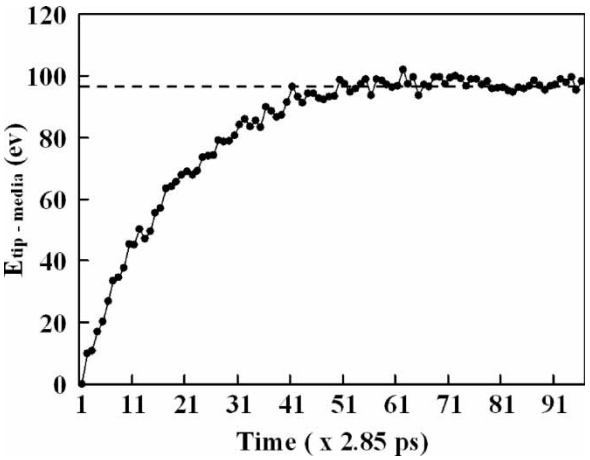

Figure 6. Energy transferred from nano-tip to storage medium film at different time.

The heat transformation from the nano-tip to the medium film is also simulated. In this study, the nano-tip touches with the medium film without external force. The temperature of nano-tip is kept constant at 500 K and the initial temperature of medium film is 300 K before the heat transfer process. The snapshots of temperature distribution in medium film surface during heat transfer are shown in Figure 4. The characteristic size of the heated zone in contact is a square of edge $3\sqrt{2}a_0$. As shown in Figure 4a, at beginning, the geometry of the heat flux reproduces the square shape of the nano-tip projection. After a short time, the imprint of the nano-tip becomes unsymmetrical, as shown in Figure 4(b)–(d). This phenomenon coincides with the characteristic of the medium film, which is amorphous with different thermal properties in different directions.

Figure 5 reports the temperature profiles at the middle section of the medium film along the x direction at different time. It can be observed that when the system reaches steady state, there is almost no thermal resistance over the interface between the nano-tip and the medium film. This is because they are the same silicon material. The steady heat flux ($J_z = E_{\text{tip-media}}/A\Delta t = 1.03 \times 10^{12}$ J/m^{2}s) from the nano-tip to the medium film can be obtained according to Figure 6, where $E_{\text{tip-media}} = 97.0$ eV, $A = 5.31$ nm^2 and $\Delta t = 2.85$ ps. It can be observed that when the time is in the order of 0.11 ns, the system reaches equilibrium status, and about 95.5 nm^2 area is heated to 500 K. This time period is much smaller than the conduction timescale (2 μs) on the tip in the heat-assisted scanning probe-based data storage technology during data bit recording process [2], where data bit sizes are about 10–50 nm in diameter, the tip-medium contact zone at the beginning of writing process is about 10–40 nm^2. Our simulation results indicate that at the beginning of writing process, the nano-tip can transfer sufficient heat energy to soften the medium film, thus helping to alleviate nano-tip wear during the indentation process.

5. Conclusion

The thermal properties of nano-tip have been investigated by the NEMD simulation. Obvious structural configuration and boundary condition effects on the thermal transport have been observed due to the phonon boundary-scattering and possible phonon spectrum modification. Moreover, the thermal conductivity of the nano-tip has been calculated. The results provide some insights for the future design optimization of the nano-tip structures. The heat transformation from the nano-tip to the silicon medium film is also simulated, which provides constructive information about heating time, energy

transferred and heated medium area in the data writing process. This study builds up the foundation for the study of nano-indentation with heat transfer between the tips and other different medium materials (e.g. metal, magnetic and polymer) in the thermal-assisted data storage technologies.

Notes

1. Email: liux0014@ntu.edu.sg
2. Email: yang_jiaping@dsi.a-star.edu.sg

References

[1] R.E. Rottmayer, S. Batra, D. Buechel, W.A. Challener, J. Hohlfeld, Y. Kubota, L. Li, B. Lu, C. Mihalecea, K. Mountfield, K. Pelhos, C.B. Peng, T. Rausch, M.A. Seigler, D. Weller, and X.M. Yang, *Heat-assisted magnetic recording*, IEEE Trans. Magnet. 42 (2006), p. 2417.
[2] G. Binning, M. Despont, U. Drechsier, W. Haberle, M. Lutwyche, P. Vettiger, H.J. Mamin, B.W. Chui, and T.W. Kenny, *Ultrahigh-density atomic force microscopy data storage with erase capability*, Appl. Phys. Lett. 76 (1999), p. 1329.
[3] P. Vettiger, G. Cross, M. Despont, U. Drechsler, U. Durig, B. Gotsmann, W. Haberle, M.A. Lantz, H.E. Rothuizen, R. Stutz, and G.K. Bing, *The "Millipede"—nanotechnology entering data storage*, IEEE Trans. Nanotechnol. 1 (2002), p. 39.
[4] S. Gidon, O. Lemonnier, B. Rolland, O. Bichet, C. Dressler, and Y. Samson, *Electrical probe storage using Joule heating in phase change media*, Appl. Phys. Lett. 85 (2004), p. 6392.
[5] J.P. Yang, *MEMS-based probe recording technology*, J. Nanosci. Nanotechnol. 7 (2007), p. 181.
[6] D.G. Cahill, W.K. Ford, K.E. Goodson, G.D. Mahan, A. Majumdar, H.J. Maris, R. Merlin, and S.R. Phillpot, *Nanoscale thermal transport*, J. Appl. Phys. 93 (2003), p. 793.
[7] J. Tersoff, *New empirical approach for the structure and energy of covalent systems*, Phys. Rev. B 37 (1988), p. 6991.
[8] J. Tersoff, *Empirical interatomic potential for silicon with improved elastic properties*, Phys. Rev. B 38 (1988), p. 9902.
[9] C. Kittel, *Introduction to Solid State Physics*, Vol. 90, 8th edn, Wiley, New York, 2005.
[10] A. Maiti, G.D. Mahan, and S.T. Pantelides, *Dynamical simulations of nonequilibrium processes—heat flow and the Kapitza resistance across grain boundaries*, Solid State Commun. 102 (1997), p. 517.
[11] B. Diu, C. Guthmann, D. Lederer, and B. Roulet, *Elements de Physique Statistique*, Vol. 1002, Hermann, Paris, 1989.
[12] P. Jund, and R. Jullien, *Molecular-dynamics calculation of the thermal conductivity of vitreous silica*, Phys. Rev. B 59 (1999), p. 13707.